The current issue and full text archive of this journal is available on Emerald Insight at:
https://www.emerald.com/insight/1756-8692.htm

Near-zero carbon stochastic dispatch optimization model for power-to-gas-based virtual power plant considering information gap status theory

Received 14 February 2022
Revised 25 February 2022
Accepted 8 March 2022

Liwei Ju, Zhe Yin, Qingqing Zhou, Li Liu, Yushu Pan and Zhongfu Tan
North China Electric Power University, Beijing, China

Abstract

Purpose – This study aims to form a new concept of power-to-gas-based virtual power plant (GVPP) and propose a low-carbon economic scheduling optimization model for GVPP considering carbon emission trading.

Design/methodology/approach – In view of the strong uncertainty of wind power and photovoltaic power generation in GVPP, the information gap decision theory (IGDT) is used to measure the uncertainty tolerance threshold under different expected target deviations of the decision-makers. To verify the feasibility and effectiveness of the proposed model, nine-node energy hub was selected as the simulation system.

Findings – GVPP can coordinate and optimize the output of electricity-to-gas and gas turbines according to the difference in gas and electricity prices in the electricity market and the natural gas market at different times. The IGDT method can be used to describe the impact of wind and solar uncertainty in GVPP. Carbon emission rights trading can increase the operating space of power to gas (P2G) and reduce the operating cost of GVPP.

Research limitations/implications – This study considers the electrical conversion and spatio-temporal calming characteristics of P2G, integrates it with VPP into GVPP and uses the IGDT method to describe the impact of wind and solar uncertainty and then proposes a GVPP near-zero carbon random scheduling optimization model based on IGDT.

Originality/value – This study designed a novel structure of the GVPP integrating P2G, gas storage device into the VPP and proposed a basic near-zero carbon scheduling optimization model for GVPP under the optimization goal of minimizing operating costs. At last, this study constructed a stochastic scheduling optimization model for GVPP.

Keywords Virtual power plant, Information gap, Power-to-gas, Near-zero carbon, Stochastic dispatching

Paper type Research paper

© Liwei Ju, Zhe Yin, Qingqing Zhou, Li Liu, Yushu Pan and Zhongfu Tan. Published by Emerald Publishing Limited. This article is published under the Creative Commons Attribution (CC BY 4.0) licence. Anyone may reproduce, distribute, translate and create derivative works of this article (for both commercial and non-commercial purposes), subject to full attribution to the original publication and authors. The full terms of this licence may be seen at http://creativecommons.org/licences/by/4.0/legalcode

This work was partially supported by the Beijing Social Science Fundation (21JCC088).

Declaration of competing interest: The authors declare that they have no known competing financial interests or personal relationships that could have appeared to influence the work reported in this study.

International Journal of Climate Change Strategies and Management
Vol. 15 No. 2, 2023
pp. 105-127
Emerald Publishing Limited
1756-8692
DOI 10.1108/IJCCSM-02-2022-0018

Nomenclature Abbreviations

GVPP = power-to-gas-based VPP;
PV = photovoltaic;
IGDT = information gap decision theory;
GSD = gas storage device;
P2G = power-to-gas;
GST = gas storage tank;
WPP = Wind power plant;
PSD = power storage device;
DRP = demand response provider;
CGT = conventional gas turbine;
BPG = biomass power generation;
UPG = utility power grid;
GAMS = the general algebraic modeling system; and
CGT = mixed integer linear programming.

Set

t = index for time; and
j = index for step.

Scalar

$Q_{\mathrm{P2G}}^{\mathrm{rated}}$ = rated gas production power of P2G;
α = maximum degree of uncertainty;
δ = carbon emissions per unit of electricity;
$\boldsymbol{\eta}_{CGT,t}$ = conversion efficiency of natural gas;
$\boldsymbol{\eta}_{BPG,t}$ = conversion efficiency of biomass fuel;
$\boldsymbol{\lambda}$ = government or the regulatory authority sets the carbon emission reduction allocation rate;
a = calculation coefficients of carbon emissions from CGT power generation;
b = calculation coefficients of carbon emissions from biomass power generation(BPG) power generation;
c = calculation coefficients of carbon emissions from utility power grid (UPG) power generation;
$\boldsymbol{d}$ = length of the carbon emission growth interval;
$\boldsymbol{\sigma}$ = increase of the carbon trading price of each step;
$\boldsymbol{\eta}$ = price range of the carbon emission;
a_{CGT} = calculation coefficients of CGT power generation fuel cost;
b_{CGT} = calculation coefficients of CGT power generation fuel cost;
c_{CGT} = calculation coefficients of CGT power generation fuel cost; and
σ_{risk} = expected target deviation coefficient.

Parameter

$C_{\mathrm{CO_2}}$ = carbon trading cost of GVPP;
$P_{\mathrm{CO_2}}$ = carbon trading price on the market;
$P_{UPG,t}$ = price of electricity purchased;
$C_{CGT,t}$ = power generation cost of CGT at time t;
$C_{BPG,t}$ = power generation cost of BPG at time t;
$C_{CGT,t}^{\mathrm{sd}}$ = start and stop cost of CGT at time t;
N_{CGT}^{hot} = hot start cost of CGT;
N_{CGT}^{cold} = cold start cost of CGT;

N_{CGT}^{off} = shutdown cost of CGT;
$Q_{\mathrm{P2G},t}$ = natural gas production by P2G at time t;
S_{GST,T_0} = gas storage in GST at the initial moment;
$Q_{\mathrm{GST},t}^{\mathrm{P2G}}$ = the amount of natural gas entering GST at time t;
$Q_{\mathrm{GST},t}^{\mathrm{CGT}}$ = the amount of natural gas that GST inputs to CGT at time t;
$Q_{\mathrm{GST},t}^{\mathrm{CH_4}}$ = the amount of natural gas that GST enters the natural gas network at time t;
$S_{\mathrm{GST},t}^{\max}$ = maximum gas storage capacity of GST at time t;
$S_{\mathrm{GST},t}^{\min}$ = minimum gas storage capacity of GST at time t;
$Q_{\mathrm{GST},t}^{\mathrm{P2G,min}}$ = minimum power of the gas storage of GST at time t;
$Q_{\mathrm{GST},t}^{\mathrm{P2G,max}}$ = maximum power of the gas storage of GST at time t;
$Q_{\mathrm{P2G},t}^{\min}$ = minimum power of natural gas output by P2G at time t;
$Q_{\mathrm{P2G},t}^{\max}$ = maximum power of natural gas output by P2G at time t;
$Q_{\mathrm{GST},t}^{\min}$ = minimum power of natural gas output by GST at time t;
$Q_{\mathrm{GST},t}^{\max}$ = maximum power of natural gas output by GST at time t;
$g_{CGT}^{\max}$ = maximum power generation of CGT;
$g_{CGT}^{\min}$ = minimum power generation of CGT;
Δg_{CGT}^{+} = up climbing power of CGT;
Δg_{CGT}^{-} = down climbing power of CGT;
M_{CGT}^{on} = shortest starting time of CGT;
M_{CGT}^{off} = shortest downtime of CGT;
$g_{PSD,t}^{\max}$ = maximum charge and discharge power of the PSD at time t, respectively;
$g_{PSD,t}^{\min}$ = minimum charge and discharge power of the PSD at time t, respectively;
$E_{\mathrm{CO_2},t}^{P2G}$ = carbon emissions that can be converted by P2G;
$S_{PSD,t}^{\max}$ = maximum power storage capacity of the PSD at time t;
$S_{PSD,t}^{\min}$ = minimum power storage capacity of the PSD at time t;
$S_{PSD,t+1}$ = storage capacity of the PSD at time t+1;
$D^{j,\min}$ = minimum power generation output provided by DRP at step j;
D_t^j = power generation output that DRP can provide at step j at time t;
$\Delta L_{DRP,t}^{\max}$ = maximum power generation output allowed by DRP at time t;
$g_{GVPP,t}^{\max}$ = maximum and minimum output power of GVPP at time t;
$g_{GVPP,t}^{\min}$ = maximum and minimum output power of GVPP at time t;
$g_{PSD,t}^{\mathrm{dis,max}}$ = maximum discharge power of the PSD at time t;
$g_{PSD,t}^{\mathrm{chr,max}}$ = maximum charge power of the PSD at time t;
$P_{R,t}$ = peak shaving cost of wind power and PV in response to power deviation at time t;
$\boldsymbol{g}_t$ = output state of traditional power generation resources other than wind and solar at time t;
$\boldsymbol{u}_t$ = start-stop state of traditional power generation resources other than wind and solar at time t;
$T_{CGT,t}^{\mathrm{on}}$ = continuous running time of CGT at time t;
$T_{CGT,t}^{\mathrm{off}}$ = down time of CGT at time t;
$T_{CGT}^{\min}$ = shortest hot start time of CGT;
T_{CGT}^{cold} = cold start time of CGT;

$T_{CGT}^{off,\min}$ = down time of CGT;
$T_{CGT,t-1}^{on}$ = continuous running time of CGT at t − 1;
$T_{CGT,t-1}^{off}$ = continuous downtime of CGT at t − 1;
$\eta_{PSD,t}^{chr}$ = charge power of the PSD at time t;
$\eta_{PSD,t}^{dis}$ = discharge power of the PSD at time t;
$\eta_{PSD,t}^{chr}$ = charge power of the PSD at time t;
$\eta_{PSD,t}^{dis}$ = discharge power of the PSD at time t; and
$\tilde{E}$ = free carbon emission quota obtained by GVPP.

Variables

$g_{CGT,\,t}$ = power generation of CGT at time *t*;
$g_{BPG,t}$ = power generation of BPG at time t;
$g_{UPG,t}$ = purchased electricity of GVPP at time t;
E = actual carbon emissions of GVPP;
$g_{CGT,t}^{P2G}$ = power generation of CGT using methane provided by P2G at time *t*;
$g_{CGT,t}^{GST}$ = power generation of CGT using methane provided by GST at time *t*;
$g_{PSD,t}^{chr}$ = charging power of energy storage at time t;
$g_{UPG,t}$ = outsourced power output of GVPP at time t;
$\Delta L_{DRP,t}$ = output provided by the demand response integrator (DRP) at time t;
L_t = load demand at time t;
$\Delta L_{P2G,t}$ = power load of P2G at time t;
ΔL_t^j = actual power generation output provided by DRP at step j at time t;
F_{cost} = operating cost of GVPP;
$g_{UPG,t}$ = electricity purchased by GVPP at time t;
$u_{CGT,t}$ = operating state of CGT at time t;
$g_{PV,t}$ = power generation output of PV at time t;
$g_{WPP,t}$ = power generation output of WPP at time t;
$g_{PSD,t}^{dis}$ = discharging power of energy storage at time t;
$g_{WPP,t}^{*}$ = actual output power generation of wind power;
$g_{PV,t}^{*}$ = actual output power generation of PV;
F_{risk} = expected target value of the decision-maker;
$F_{\text{cost}}^{\text{opt}}$ = optimal GVPP target value;
$L_{\text{net},t}$ = net load demand at time *t*; and
S_{swort} = the worst scenario of GVPP operation.

1. Introduction

In recent years, resource and environmental constraints have been continuously strengthened, and the centralized energy development model has gradually become difficult to meet the requirements of transmission loss, utilization efficiency and environmental pollution. Distributed energy with gold users and high-efficiency has developed rapidly. In the "13th Five-Year Plan for Energy," it is specified that the installed capacity of distributed natural gas power generation and photovoltaic (PV) power generation will reach 15 million kilowatts and 60 million kilowatts by the end of 2020 and actively develop decentralized wind power [1]. However, the small-capacity, large-volume and low-density characteristics of distributed energy sources have caused their large-scale access to bring great challenges to the safe and stable operation of the power grid.

Virtual power plant (VPP) uses advanced intelligent computer technology and communication systems to aggregate a variety of distributed power sources, energy storage and flexible loads, etc., to achieve the goal of overall participation in the optimal operation of the power system (Ju *et al.*, 2019a). In particular, the power-to-gas (P2G) technology is becoming more and more mature, which can use electric energy to convert CO_2 into methane to achieve flexible electrical conversion (Götz *et al.*, 2016). If it is combined with VPP to P2G-based VPP (GVPP), it will generate electricity-gas-electricity recycling utility and carbon emission reduction effect. It has important theoretical value and practical significance for promoting the optimized utilization of distributed energy and the clean, low-carbon, efficient and safe utilization of energy.

Many researches have been carried out on the optimization of distributed energy utilization with P2G at home and abroad. The main operating process of P2G includes two processes: water electrolysis and methanation. Water electrolysis process splits water into hydrogen and oxygen by using electricity. Methanation is the chemical reaction of hydrogen and CO_2 to produce CH_4, and the consumption and production of water in the two processes are equal (Guandalini *et al.*, 2015). Paolo *et al.* (2018) established an electrical interconnection system with P2G and proposed the concept of energy flow that integrates electricity and natural gas. Manuel *et al.* (2018) established a P2G-containing power system scheduling optimization model with strong versatility and scalability and analyzed the application space of P2G from the level of large-scale power systems. Furthermore, David *et al.* (2018) discussed the cooperative operation of P2G and distributed energy, established a P2G-containing multi-source microgrid operation optimization model and analyzed the effect of P2G on the utilization of distributed energy. Chaudry *et al.* (2008) build a P2G-containing multi-level energy system scheduling model and discuss the optimization effect of P2G technology in improving system operation economy and reducing natural gas node pressure. The abovementioned research provides a prerequisite foundation for the construction of the optimal operation model of GVPP. However, the existing literature seldom considers the fusion effect of P2G and carbon emissions trading and only considers the problems of P2G's own operating costs and system economics. In fact, China's unified carbon trading market has been launched, and the eight pilot projects carried out in the early stage have completed a considerable transaction scale (Wang *et al.*, 2019). If carbon emission rights trading and P2G can be combined with each other, and the optimization of GVPP operation is considered, it will help to improve the economic and environmental benefits of GVPP operation, and it will also help promote the market to absorb distributed clean energy enthusiasm (Liu *et al.*, 2021). Based on the analysis, this study focuses on the research of GVPP scheduling optimization in the context of carbon emissions trading.

In addition, in the GVPP with random distributed power sources such as wind, how to analyze the influence of wind and solar uncertainty is also a key issue for the optimization of GVPP. Existing research results are mainly divided into probabilistic decision-making methods (Aien *et al.*, 2016) and fuzzy decision-making methods (Aguilar *et al.*, 2021). Majidi *et al.* (2019) calculate the spinning reserve capacity under the condition of certain risk probability according to the probabilistic wind power, conventional unit shutdown and load uncertainty. Compared with the probability decision method, the fuzzy decision method does not need the probability distribution function of random variables but uses the membership function to fuzzify the uncertain variables. Wang *et al.* (2020) propose a robust standby dispatch mode and a robust economic dispatch mode for multiple scenarios of wind power. Among the above two types of methods, how the first type of method accurately obtains the probability distribution function of the uncertainty variable has become a key constraint affecting the accuracy of the decision result. The second type of method does not need to establish the probability distribution of the uncertainty variable but needs to make subjective simple assumptions, which makes it difficult to set the subjective and objective fuzzy rules and membership functions reasonably. However,

the information gap decision theory (IGDT) theory can maximize the unfavorable disturbance of uncertain variables under the premise of meeting the pre-set target requirements. The obtained solution can be guaranteed not to be worse than the preset target within the perturbation range (Pilar *et al.*, 2018) and can overcome the shortcomings of the above two types of methods. In this study, it is used to describe the wind-solar uncertainty in GVPP and construct the GVPP stochastic scheduling optimization model.

Based on the above analysis, domestic and foreign scholars have carried out a series of GVPP optimization operation research and put forward research results that meet the decision-making requirements in terms of system configuration, uncertainty analysis, optimized operation model and benefit distribution strategy. However, it should be noted that there are some gaps in previous research. On the one hand, for VPP, conventional gas turbine (CGT) units have become an indispensable and important component of VPP due to their fast start and stop speeds and low power generation emissions. P2G can convert the CO_2 generated by the CGT power generation to CH_4 by using the abandonment of wind and the amount of abandonment of electricity, and it can be used by the CGT for power generation again. This can reduce the carbon emissions of VPP operations, but the existing literature seldom considers the fusion effect of P2G and carbon emission rights trading and only considers the problems of P2G's own operating costs and system economics. On the other hand, due to the large uncertainty in wind power plant (WPP) and PV power generation, when P2G is integrated into VPP, the impact of uncertainty will extend from the power system to the natural gas system. However, the current two main uncertainty analysis methods have their own shortcomings. The IGDT can maximize the unfavorable disturbance of uncertain variables under the premise of meeting the requirements of the preset target, and the obtained solution can be guaranteed to be no worse than the preset target within the range of the disturbance. Therefore, all the above analysis motivates us to put forward an optimization scheduling model of the GVPP. The main contributions of this study are summarized as follows:

- design a novel structure of GVPP integrating P2G, gas storage equipment (GSD) into the VPP. VPP includes WPP, PV, CGT, power storage device (PSD) and controllable load;
- proposed a basic near-zero carbon scheduling optimization model for GVPP under the optimization goal of minimizing operating costs, considering constraints such as power supply and demand balance, P2G–GST joint operation, energy storage equipment operation and spinning reserve. This model can be used to calculate the expected optimization goals of decision-makers and provide a prerequisite basis for the establishment of stochastic scheduling optimization models; and
- construct a stochastic scheduling optimization model for GVPP by using the IGDT to measure the uncertainty tolerance threshold under different expected target deviations and to establish the near-zero carbon emission stochastic scheduling optimization model for GVPP under the standard and the worst scenarios.

The rest of this study is organized as follows. Section 1 designs a novel structure of GVPP and calculated the carbon transaction cost of GVPP. Then, in Section 2, the near-zero carbon scheduling optimization model for GVPP is constructed. In Section 3, application of the IGDT is used to construct a stochastic scheduling optimization model considering the uncertainty of WPP and PV. Finally, in Section 4 the nine-node energy hub system is selected as the simulation system for verifying the effectiveness and applicability of the proposed model. Section 5 highlights the contributions and conclusions of the Section 1 system structure and carbon transaction cost model.

1.1 Power-to-gas-based virtual power plant system composition

GVPP integrates P2G devices and gas storage tank (GST) with conventional VPP distributed energy sources such as WPP, PV station, CGT, PSD and controllable loads. Among them, the controllable load participates in system dispatch through an incentive demand response method, which is mainly provided by a demand response provider (DRP) and is generally industrial loads with flexible power characteristics, electric vehicle loads and some commercial loads. PSD and GSD are based on real-time electricity price and gas price, choose discharge/gas or charge/gas, so as to earn "spread" income. Figure 1 is a schematic diagram of the structure of GVPP.

In GVPP, P2G operations are divided into two processes: electrolysis and methanation. Electrolysis is the direct injection of hydrogen into natural gas pipelines or hydrogen storage equipment after the excess electric energy is produced by electrolyzing water to produce hydrogen, and its energy conversion efficiency can reach 75% to 85%. The methanation process is based on electrolysis. Under the action of a catalyst, the hydrogen and carbon dioxide generated by the electrolysis of water react to form methane and water. The specific chemical reactions are as follows:

$$2H_2O \overset{\text{electrolysis}}{\rightarrow} 2H_2 + O_2 \tag{1}$$

$$CO_2 + 4H_2 \rightarrow CH_4 + 2H_2O \tag{2}$$

Through the abovementioned two-stage chemical reaction, the comprehensive efficiency of electricity-to-natural gas conversion is between 45% and 60%. After the electricity is converted into natural gas, it can be injected into a natural gas network or GSD. It can be seen that the H_2O input and output of the P2G chemical reaction are the same, and only CO_2 is consumed, which is conducive to reducing the carbon emissions of GVPP power generation. Figure 2 is a schematic diagram of P2G technology.

1.2 Power-to-gas-based virtual power plant carbon transaction costs

Carbon trading is a trading mechanism that allows participants to trade carbon emissions as commodities by establishing a fair, open and just carbon trading market, thereby achieving the goal of systematic carbon emission reduction (Geert *et al.*, 2018). Generally speaking, the allocation of carbon emission allowances is mainly based on free allocation. All participating

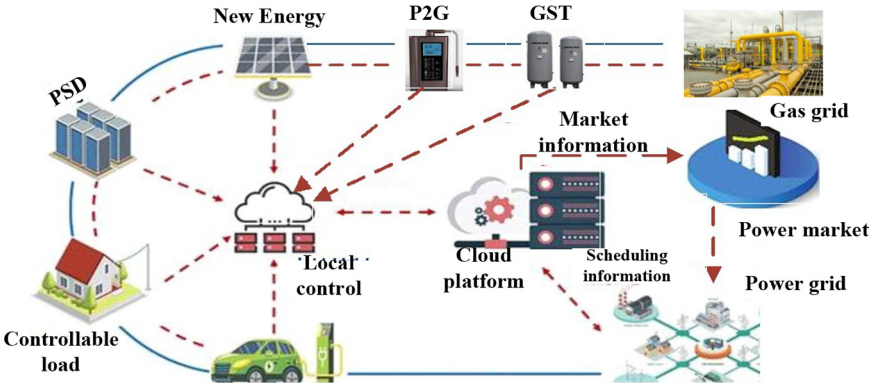

Figure 1.
Composition diagram of VPP

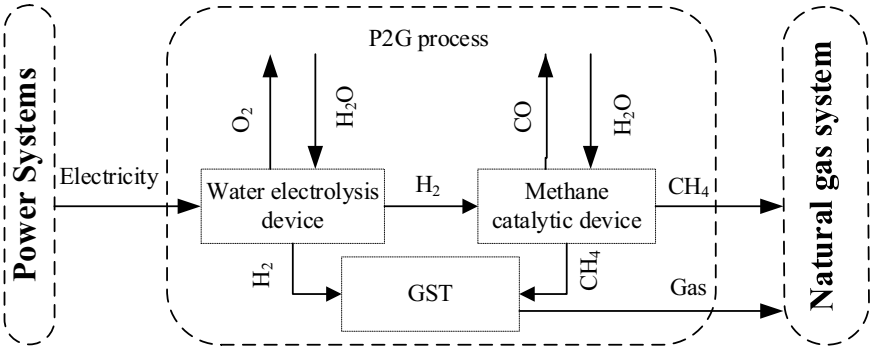

Figure 2.
Technology schematic of P2G

entities formulate and adjust production plans based on the carbon emission allowances they have obtained. If the actual carbon emissions are higher than the allocated allowances, they need to purchase excess shares in the carbon trading market. On the contrary, the remaining allowances can be sold in the carbon trading market. For GVPP, the initial free carbon emission allowance is directly related to the power generation of different components, and carbon trading can be carried out for the excess or deficiency. GVPP carbon emission sources include two channels, namely traditional power generation resources and purchased power. Among them, traditional power generation resources include gas-fired power generation and biomass fuel power generation. At the same time, for the convenience of analysis, it is assumed that the electricity purchased by GVPP is thermal power. At this time, the carbon emission allowances obtained by GVPP is calculated as follows:

$$\tilde{E} = \sum_{t=1}^{T} \delta(1-\lambda)(\eta_{CGT,t} g_{CGT,t} + \eta_{BPG,t} g_{BPG,t} + g_{UPG,t})\Delta t \tag{3}$$

where δ refer to Geert *et al.* (2018), set to 0.648; further, to calculate the carbon emission cost of GVPP, it is necessary to calculate the actual carbon emission of GVPP. According to the Ju *et al.* (2019a), the carbon emission of CGT and BPG power generation is actually a quadratic function, and the specific calculation is as follows:

$$E = \sum_{t=1}^{T}\left[a_1 + b_1\left(g_{CGT,t} + g_{CGT,t}^{P2G} + g_{CGT,t}^{GST}\right) + c_1\left(g_{CGT,t} + g_{CGT,t}^{P2G} + g_{CGT,t}^{GST}\right)^2\right] - E_{CO_2,t}^{P2G} + \sum_{t=1}^{T}\left[a_2 + b_2 g_{BPG,t} + c_2 g_{BPG,t}^2\right] + \sum_{t=1}^{T}\left[a_3 + b_3 g_{UPG,t} + c_3 g_{UPG,t}^2\right] \tag{4}$$

where $E_{CO_2,t}^{P2G}$ is a carbon emission reduction.

To perform differentiated cost accounting for different carbon emission statuses, drawing on the ideas of Geert *et al.* (2018), constructing a stepped carbon transaction cost calculation model, based on the free carbon emissions calculated in formula (3), divide a number of different carbon emission ranges. When the carbon emissions are higher, the carbon trading settlement price is also higher. The calculation formula of GVPP ladder carbon transaction cost is as follows:

$$C_{CO_2}=\begin{cases} P_{CO_2}(E-\tilde{E}) & ,\tilde{E}\le E+d \\ \sigma P_{CO_2}d+(1+\sigma)P_{CO_2}(E-\tilde{E}-d), & E+d\le\tilde{E}\le E+2d \\ (2+\sigma)P_{CO_2}d+\left[(1+2\sigma)P_{CO_2}(E-\tilde{E}-2d)\right], & E+2d\le\tilde{E}\le E+3d \\ \quad\vdots & \\ (n-1+\sigma)P_{CO_2}d+\left[(1+(n-1)\sigma)P_{CO_2}\left(E-\tilde{E}-(n-1)d\right)\right], & E+(n-1)d\le\tilde{E}\le E+nd \end{cases} \tag{5}$$

When $E,\tilde{E}$, C_{CO_2} is a negative value, indicating that the actual carbon emissions of the system will be lower than the free carbon emissions. At this time, the initial carbon trading price can be purchased and stored to obtain carbon trading benefits.

2. Near-zero carbon scheduling optimization model

2.1 Objective function

Considering that GVPP participates in power system dispatch as a whole, that is, it is a low-carbon economic dispatch optimization problem 24 h before the day. According to formula (4), if $E = 0$ at the end of the scheduling period, it indicates that all the CO_2 generated by GVPP is converted into CH_4, which enters the gas network or is stored in the GST. It is considered that GVPP has achieved the goal of zero carbon emissions. However, zero carbon emissions requires P2G to fully use clean energy to generate electricity and convert CO_2 in the last period of the dispatch cycle, which is difficult to achieve. Therefore, this study pursues the goal of near-zero carbon emissions, considering the maximum value of $E\rightarrow 0$, the carbon transaction cost is as small as possible. At the same time, the operating cost of GVPP also includes the cost of power generation fuel and the cost of outsourcing electricity. Therefore, this study chooses to minimize the operating cost as the optimization objective. The specific objective function is as follows:

$$F_{\text{cost}}=\min\sum_{t=1}^{T}\left(C_{CO_2,t}+C_{CGT,t}+C_{BPG,t}+P_{UPG,t}g_{UPG,t}\right) \tag{6}$$

where $C_{CGT,t}$ and $C_{BPG,t}$ mainly include fuel cost and start-up and stop cost. Taking CGT as an example, the specific calculation is as follows:

$$C_{CGT,t}=\left[a_{CGT}+b_{CGT}g_{CGT,t}+c_{CGT}(g_{CGT,t})^2\right]+C^{\text{sd}}_{CGT,t} \tag{7}$$

$$C^{\text{sd}}_{CGT,t}=\left[u_{CGT,t}\left(1-u_{CGT,t-1}\right)\right]\times\begin{cases} N^{hot}_{CGT},\ T^{\min}_{CGT}<T^{\text{off}}_{CGT,t}\le T^{\min}_{CGT}+T^{cold}_{CGT} \\ N^{cold}_{CGT},\ T^{\text{off}}_{CGT,t}>T^{\min}_{CGT}+T^{cold}_{CGT} \end{cases}+$$

$$\left[u_{CGT,t-1}\left(1-u_{CGT,t}\right)\right]\times\begin{cases} N^{off}_{CGT},\ T^{\text{on}}_{CGT,t}\ge T^{off,\min}_{CGT} \\ 0,\ T^{\text{on}}_{CGT,t}<T^{off,\min}_{CGT} \end{cases} \tag{8}$$

2.2 Constraint conditions

In the process of GVPP operation, it is necessary to consider the load supply and demand balance constraints, the operation of each component unit and the spinning reserve constraints. The specific constraints are as follows.

2.2.1 Load supply and demand balance constraint.

$$g_{WPP,t} + g_{PV,t} + g_{CGT,t} + g_{CGT,t}^{P2G} + g_{CGT,t}^{GST} + g_{BPG,t} + \left(g_{PSD,t}^{dis} - g_{PSD,t}^{chr}\right) + \Delta L_{DRP,t} + g_{UPG,t} = L_t + \Delta L_{P2G,t} \tag{9}$$

where $g_{PV,t}$ and $g_{WPP,t}$ mainly depend on the natural wind and solar radiation intensity. For specific calculations, see reference (Götz *et al.*, 2016).

2.2.2 Power-to-gas–gas storage tank joint operation constraints.

$$0 \le Q_{\mathrm{P2G},t} \le Q_{\mathrm{P2G}}^{\mathrm{rated}} \tag{10}$$

$$Q_{\mathrm{GST},t}^{\mathrm{P2G,min}} \le Q_{\mathrm{GST},t}^{\mathrm{P2G}} \le Q_{\mathrm{GST},t}^{\mathrm{P2G,max}} \tag{11}$$

$$Q_{\mathrm{P2G},t}^{\min} \le Q_{\mathrm{P2G},t}^{\mathrm{CH_4}} + g_{CGT,t}^{\mathrm{P2G}} / \varphi_{\mathrm{CGT}} \mathrm{H_g} \le Q_{\mathrm{P2G},t}^{\max} \tag{12}$$

$$Q_{\mathrm{GST},t}^{\min} \le Q_{\mathrm{GST},t}^{\mathrm{CH_4}} + g_{\mathrm{CGT},t}^{\mathrm{GST}} / \varphi_{\mathrm{CGT}} \mathrm{H_g} \le Q_{\mathrm{GST},t}^{\max} \tag{13}$$

$$S_{\mathrm{GST},t} = S_{\mathrm{GST},T_0} + \sum_{t=1}^{T} \left(Q_{\mathrm{GST},t}^{\mathrm{P2G}} - Q_{\mathrm{GST},t}^{\mathrm{CGT}} - Q_{\mathrm{GST},t}^{\mathrm{CH_4}}\right) \tag{14}$$

$$S_{\mathrm{GST},t}^{\min} \le S_{\mathrm{GST},t} \le S_{\mathrm{GST},t}^{\max} \tag{15}$$

2.2.3 Conventional gas turbine and BPG operating constraints. Both CGT and BPG are traditional power generation resources, and their power generation needs to satisfy maximum output power constraints, up and down climbing power constraints and start-stop time constraints. Take CGT as an example, the details are as follows:

$$u_{CGT,t} g_{CGT}^{\min} \le g_{CGT,t} \le u_{CGT,t} g_{CGT}^{\max} \tag{16}$$

$$\Delta g_{CGT}^{-} \le g_{CGT,t} - g_{CGT,t-1} \le \Delta g_{CGT}^{+} \tag{17}$$

$$\left(T_{CGT,t-1}^{\mathrm{on}} - M_{CGT}^{\mathrm{on}}\right)\left(u_{CGT,t-1} - u_{CGT,t}\right) \ge 0 \tag{18}$$

$$\left(T_{CGT,t-1}^{\mathrm{off}} - M_{CGT}^{\mathrm{off}}\right)\left(u_{CGT,t} - u_{CGT,t-1}\right) \ge 0 \tag{19}$$

2.2.4 Energy storage equipment operation constraints. The operation of energy storage equipment needs to consider the maximum charge and discharge power constraints and its own battery capacity constraints. The specific constraints are as follows:

$$g_{PSD,t}^{\min} \le g_{PSD,t} \le g_{PSD,t}^{\max} \tag{20}$$

$$S_{PSD,t}^{\min} \le S_{PSD,t} \le S_{PSD,t}^{\max} \tag{21}$$

$$S_{PSD,t+1} = S_{PSD,t} + \left[g_{PSD,t}^{chr}\left(1 - \eta_{PSD,t}^{\mathrm{chr}}\right) - g_{PSD,t}^{\mathrm{dis}} \Big/ \left(1 - \eta_{PSD,t}^{\mathrm{dis}}\right) \right] \tag{22}$$

2.2.5 Demand response provider operating constraints. This study considers that the flexible and controllable load involved in GVPP operation is mainly completed by the way that DRP provides IBDR. Generally speaking, DRP distributes demand response according to the relationship between power supply and demand. It is a multistage output method:

$$D^{j,\min} \le \Delta L_t^j \le D_t^j, j = 1 \tag{23}$$

$$0 \le \Delta L_t^j \le \left(D_t^j - D_t^{j-1}\right), j = 2, 3, \ldots, J \tag{24}$$

$$\Delta L_{DRP,t} = \sum_{j=1}^{J} \Delta L_t^j \le \Delta L_{DRP,t}^{\max} \tag{25}$$

2.2.6 Spinning reserve constraint.

$$\begin{aligned} & g_{GVPP,t}^{\max} - g_{GVPP,t} + \min\left\{ \left(g_{PSD,t}^{\mathrm{dis,max}} - g_{PSD,t}^{\mathrm{dis}}\right), \left(S_{PSD,t} - S_{PSD,t}^{\min}\right) \right\} \\ & \quad \ge r_L \cdot L_t + r_{WPP} \cdot g_{WPP,t} + r_{PV} \cdot g_{PV,t} \end{aligned} \tag{26}$$

$$\begin{aligned} & g_{GVPP,t} - g_{GVPP,t}^{\min} + \max\left\{ \left(g_{PSD,t}^{\mathrm{chr,max}} - g_{PSD,t}^{\mathrm{chr}}\right), \left(S_{PSD,t}^{\max} - S_{PSD,t}\right) \right\} \\ & \quad \ge r_{WPP} \cdot g_{WPP,t} + r_{PV} \cdot g_{PV,t} \end{aligned} \tag{27}$$

3. Stochastic scheduling optimization model

3.1 Information gap decision theory

There are uncertain variables such as wind power and PV power generation in GVPP, because its scheduling optimization decision is based on the forecast information of uncertain variables. When the actual value of the uncertainty variable deviates from the predicted value, it is considered that the uncertainty variable has an information gap. Yakov Ben-Haim *et al.* proposed and improved the IGDT in the 1980s continuously, which is used to describe the gap state between the known and unknown uncertain information

(Pilar *et al.*, 2018). When the information gap is generated, if the actual value deviates in a bad direction, it will have a negative impact on the decision-making system. Conversely, when the actual value deviates in a good direction, it will bring opportunity benefits to the decision-making system. The IGDT forms an open decision-making optimization strategy by separately constructing the risk aversion (robust) model and the risk speculation (opportunity) model corresponding to the above two directions and analyzes the degree of uncertainty and consequences, so as to formulate a more realistic decision-making plan (Pilar *et al.*, 2018). The basic model of IGDT includes system model, uncertainty model and minimum demand model, which are described as follows:

For any initial system model, it can be written in the form of objective function, inequality constraint and equality constraint, as follows:

$$\begin{cases} \min R(q,v) \\ s.t. \quad H(q,v) \le 0 \\ \qquad G(q,v) = 0 \end{cases} \tag{28}$$

where R is the objective function; q is the determined parameter; v is the uncertain parameter; $H(q, v)$ is the inequality constraint; and $G(q, v)$ is the equality constraint.

Considering the uncertainty parameter v, and its corresponding predicted value is $\tilde{v}$, the interval can be used to describe the floating state of the uncertainty variable $U(\alpha, \tilde{v})$ as follows:

$$U(\alpha,\tilde{v}) = \left\{ v(t) : \left| \frac{v(t) - \tilde{v}(t)}{\tilde{v}(t)} \right| \le \alpha \right\} \quad \alpha \ge 0 \tag{29}$$

where α is the uncertainty of the parameter v; that is, for v in the set $U(\alpha, \tilde{v})$, the maximum perturbation relative to the predicted value $\tilde{v}$ is $\alpha\tilde{v}$.

The minimum demand model is mainly used to describe the impact of the uncertainty variable predicted value deviation on the system decision. Considering that the parameter r_c is the lower limit of the target value acceptable to the decision-maker, for any parameter v, the objective function $R(q, v)$ can satisfy the following constraints:

$$R(q,v) \le r_c \tag{30}$$

According to formulas (28) to (30), the original initial system decision-making model can be transformed into an uncertain decision-making model as follows:

$$\begin{cases} \max \alpha \\ s.t. \quad R(q,v)_{v \in U(\alpha,\tilde{v})} \le r_c \\ \qquad H(q,v) \le 0 \\ \qquad G(q,v) = 0 \end{cases} \tag{31}$$

Through the abovementioned optimal model, it can be ensured that under the premise of the target value acceptable to the decision-maker, the maximum fluctuation of the uncertainty parameter can be withstood. The decision value q is obtained by formula (31), which can ensure that when v is disturbed in the set $U(\alpha, \tilde{v})$, the target value r_c acceptable to the decision-maker can be obtained.

The IGDT stochastic scheduling optimization model shown in formula (31) ensures that the obtained decision-making scheme has strong applicability, which is also called robustness, by considering the extreme situations of uncertain variables. However, the prerequisite for the optimal scheme determined by formula (36) is that the objective function changes monotonously with the wind and solar uncertainty parameters, which can be calculated by using formula (35). However, in GVPP low-carbon stochastic dispatch, when carbon transaction costs are considered, wind power and PV generation have a carbon emission reduction effect, which causes the uncertain costs of wind and solar and carbon transaction costs to offset each other. It may cause the objective function to show non-monotonic changes with the uncertainty variable; this leads to the inability to directly apply formula (35) to obtain the extreme value, the decision cost corresponding to the scene with the largest or smallest wind power is not necessarily the largest. In this case, it is necessary to establish a method for obtaining the worst scenario.

3.2 Stochastic scheduling model

This section uses IGDT to deal with the certainty of wind power and PV generation and proposes a GVPP stochastic scheduling optimization model that considers the state of information gaps. The specific process is as follows.

3.2.1 Landscape uncertainty model.

$$U(\alpha, g_{WPP,t}) = \left\{ g^{*}_{WPP,t} : \left| \frac{g^{*}_{WPP,t} - g_{WPP,t}}{g_{WPP,t}} \right| \leq \alpha \right\} \quad \alpha \geq 0 \tag{32}$$

$$U(\alpha, g_{PV,t}) = \left\{ g^{*}_{PV,t} : \left| \frac{g^{*}_{PV,t} - g_{PV,t}}{g_{PV,t}} \right| \leq \alpha \right\} \quad \alpha \geq 0 \tag{33}$$

3.2.2 Power-to-gas-based virtual power plant uncertainty decision model. According to the GVPP near-zero carbon scheduling optimization model in Section 2, the optimal GVPP target value $F^{\text{opt}}_{\text{cost}}$ under deterministic scenarios can be established, when considering the impact that uncertain variables may have on the optimal decision-making plan, according to formulas (32) and (33), the maximum perturbation of wind power and PV generation relative to the predicted value is $\alpha g_{WPP,\ t}$ and $\alpha g_{PV,\ t}$, respectively. To overcome this part of the fluctuation, GVPP needs to call conventional units or purchase electric energy from UPG, which will bring new peak shaving costs. At this time, the decision-makers expect the target value to be adjusted to:

$$F_{\text{risk}} = (1 + \sigma_{\text{risk}}) \left\{ F^{\text{opt}}_{\text{cost}} + \sum_{t=1}^{T} P_{R,t} (\alpha g_{WPP,t} + \alpha g_{PV,t}) \right\} \tag{34}$$

When the decision-maker's target value F_{risk} is higher than $F^{\text{opt}}_{\text{cost}}$, σ_{risk} takes a value greater than 0. According to formula (34), the scheduling decision value of GVPP under the uncertainty scenario should not be higher than F_{risk}, and the specific constraints are as follows:

$$\min\left[\max_{\substack{g^{*}_{WPP,t}\in U(\alpha,g_{WPP,t})\\ g^{*}_{PV,t}\in U(\alpha,g_{PV,t})}} F(g_{WPP,t},g_{PV,t},g_{DRP,t}\boldsymbol{g}_t,\boldsymbol{u}_t)\right]\le F_{\text{risk}} \tag{35}$$

Under the condition that the peak shaving transaction decision cost is not higher than the expected target F_{risk}, the maximum degree of uncertainty α is solved to establish the GVPP random scheduling decision model as follows:

$$\begin{cases}\hat{\alpha}(F_{\text{risk}})=\max\alpha\\ \min\left[\max_{\substack{g^{*}_{WPP,t}\in U(\alpha,g_{WPP,t})\\ g^{*}_{PV,t}\in U(\alpha,g_{PV,t})}} F(g_{WPP,t},g_{PV,t},g_{DRP,t}\boldsymbol{g}_t,\boldsymbol{u}_t)\right]\le F^{\text{opt}}_{\text{cost}}\\ \text{s.t. 公式 } 9-27\\ \dfrac{g^{*}_{WPP,t}-g_{WPP,t}}{g_{WPP,t}}\le\alpha\\ \dfrac{g^{*}_{PV,t}-g_{PV,t}}{g_{PV,t}}\le\alpha\end{cases} \tag{36}$$

The IGDT stochastic scheduling optimization model shown in formula (36) ensures that the obtained decision-making scheme has strong applicability, which is also called robustness, by considering the extreme situations of uncertain variables. However, the prerequisite for the optimal scheme determined by formula (36) is that the objective function changes monotonously with the wind and solar uncertainty parameters, which can be calculated by using formula (35). However, in GVPP low-carbon random scheduling, when considering carbon transaction costs, wind power and PV power generation have carbon emission reduction effects. The uncertainty cost of the scenery and the carbon transaction cost are offset by each other, which may cause the objective function to show a non-monotonic change with the uncertainty variable. This leads to the inability to directly apply formula (35) to obtain the extreme value, the decision cost corresponding to the scene with the largest or smallest wind power is not necessarily the largest. In this case, it is necessary to establish a method for obtaining the worst scenario.

3.3 Worst-case scenario analysis

Wind power and PV power generation in GVPP have strong uncertainties. When the actual output power is lower than the predicted value and the net load of the system increases rapidly, the wind and solar uncertainty will have the greatest impact on the stable operation of the system, which is the worst scenario. Therefore, it is first necessary to find the moment when the system net load fluctuates the most. The specific calculation is as follows:

$$L_{\text{net},t}=L_t+\Delta L_{P2G,t}-\left[g_{CGT,t}+g^{P2G}_{CGT,t}+g^{GST}_{CGT,t}+g_{BPG,t}+\left(g^{\text{dis}}_{PSD,t}-g^{\text{chr}}_{PSD,t}\right)+\Delta L_{DRP,t}+g_{UPG,t}\right] \tag{37}$$

$$f_t=\left\{|L_{net,t}-L_{net,t-1}|-\left[g^{\max}_{GVPP,t}-g_{GVPP,t}+\min\left\{\left(g^{\text{dis[jmath]max}}_{PSD,t}-g^{\text{dis}}_{PSD,t}\right),\left(S_{PSD,t}-S^{\min}_{PSD,t}\right)\right\}\right]\right\}\Big/L_t \tag{38}$$

According to formula (38), the net load fluctuation characteristics can be obtained, and the scenario with the largest load fluctuation is further selected as the worst scenario for GVPP operation. The specific calculation is as follows:

$$S_{swort}\left(g^{*}_{WPP,t}, g^{*}_{PV,t}\right) = \left\{ g^{*}_{WPP,t}, g^{*}_{PV,t} : \max \frac{1}{T-1} \sum_{t=2}^{T} f_t \right\} \tag{39}$$

Further, construct the GVPP scheduling optimization decision objective function corresponding to the worst scenario as follows:

$$\hat{\alpha}(F_{\text{risk}}) = \max \left\{ \alpha : \min_{\substack{g^{*}_{WPP,t} \in S_{worst} \\ g^{*}_{PV,t} \in S_{worst}}} F(g_{WPP,t}, g_{PV,t}, g_{DRP,t}\boldsymbol{g}_t, \boldsymbol{u}_t) \leq F_{\text{risk}} \right\} \tag{40}$$

According to formula (40), the GVPP system peak shaving transaction decision-making objective in the worst scenario is established, and the GVPP scheduling optimization decision-making plan obtained in this scenario is the most conservative transaction plan.

4. Case analysis

4.1 Basic data

This study chooses nine-node energy concentrator system as the simulation system, *H1* to *H9* are nine energy concentrators. Among them, *H1* is configured with 2 × 1MW WPP, *H5* is configured with 2 × 0.5 MW PV and 1 × 1MW BPG, and *H6* is configured with 1 × 1MW CGT and 1 × 1 MW·h PSD. *H7* is equipped with 1 × 0.2 MW P2G and 200 m^3 GSD. Set the maximum charge and discharge power of ESD to be 1 × 0.2 MW, the electrical energy conversion efficiency of P2G is 60%, the calorific value of natural gas is 39 MJ/m^3, and the gas storage loss rate is 5%. It is assumed that BPG power generation fuels are mainly user biogas digesters and large pig farms. The daily biogas output of a typical load is about 4746 m^3, and the relationship between biogas and output power is about 0.55–0.62 m^3/kW·h (Götz *et al.*, 2016). The power generation cost parameters and emission coefficients of CGT and BPG are selected in Ju *et al.* (2019b), and the carbon emission rights transaction price is set to 45 yuan/ton. Figure 3 is a diagram of the node energy concentrator system structure.

Furthermore, considering that WPP, PV, CGT and BPG are all dispatched by GVPP, refer to Ting *et al.* (2018) to set the on-grid power price for power generation and the price of natural gas sales for a typical load day. When GVPP cannot meet its own load demand, it can purchase electricity from UPG, and the purchase price is set at 0.8 yuan/kW·h. Using the scenario production and reduction strategy proposed in Ju *et al.* (2019a), setting the WPP and PV power generation output parameters, simulating the WPP and PV power generation scenarios of the typical load day, select the scenario with the highest probability as the input data. At the same time, considering the flexibility of end users to participate in GVPP power generation scheduling through DRP agents, the maximum positive and negative output provided by DRPs does not exceed 10% of the original load. Figure 4 shows the forecast values of wind power, PV power generation and load demand on a typical load day.

Finally, to analyze the effectiveness of IGDT in dealing with the uncertainty of WPP and PV, the initial value of the expected target deviation coefficient of decision-makers is set to 0.5, and the sensitivity analysis of the predicted deviation coefficient is performed to verify the effectiveness of the IGDT. After inputting the basic data, the model is solved by the

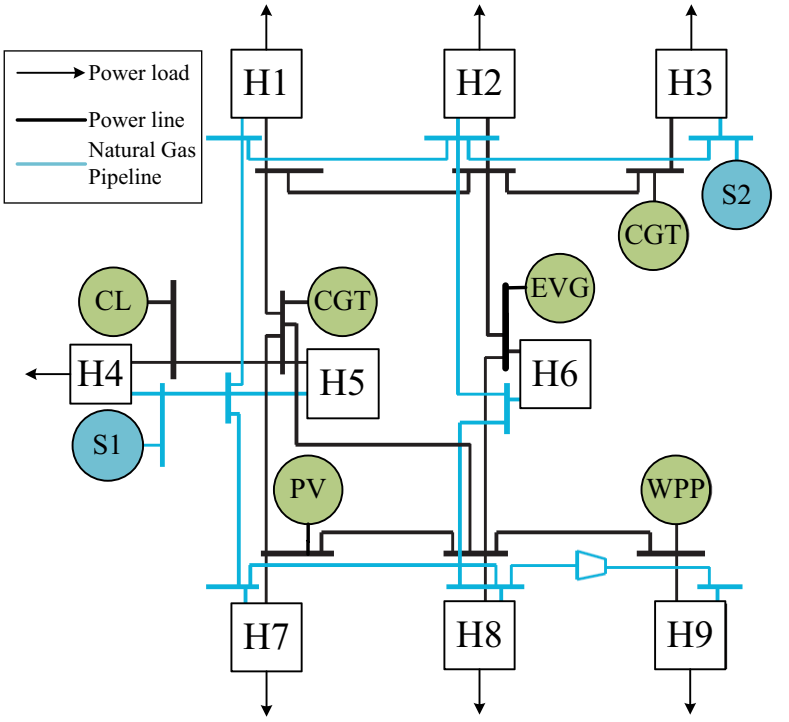

Figure 3.
Nine-node energy hub system

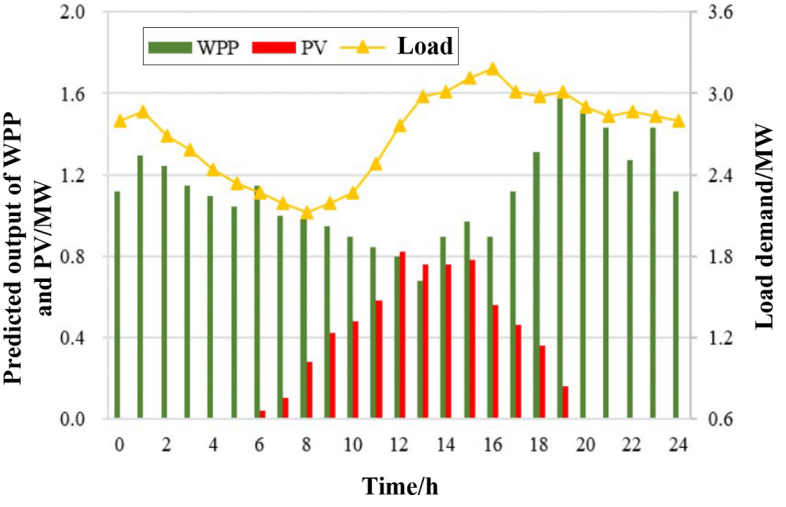

Figure 4.
Forecast values of wind power, PV power generation and load demand on typical load days

general algebraic modeling system (GAMS) software using CPLEX 11.0 linear solver from ILOG_solver (Ju *et al.*, 2019b). The CPU time required for solving the problem for different case studies with a thinkpad X1 carbon series laptop computer powered by core i5 processor and 8 GB of RAM. When the optimization is mixed integer linear programming, the GAMs software could get a satisfactory solution quickly.

4.2 Validity verification

IGDT is used to describe the optimal operation of GVPP scheduling considering the uncertainty of wind and solar, and the degree of uncertainty under different expected target deviation coefficients is measured. Overall, the degree of uncertainty has a linear relationship with the predicted target deviation coefficient, as the expected target deviation coefficient increases, that is, the increase in the cost that the decision-maker can bear, the allowable degree of uncertainty in the scenery also increases. For example, when the prediction target deviation coefficient is 0.5, the degree of uncertainty $\sigma_{\text{risk}} = 0.142$. It shows that when the wind and solar output power fluctuates within the range of [0.858, 1.142] times the predicted value, the decision-making scheme obtained by the method in this study can ensure that the cost of the dispatching decision-making scheme is less than the expected cost of the decision-maker. Figure 5 shows the relationship between the tolerance of GVPP and the expected target deviation coefficient.

Further, consider the GVPP scheduling optimization scheme in deterministic scenarios and uncertain scenarios, respectively, when $\sigma_{\text{risk}} = 0$, the decision-maker believes that the predicted value of wind and solar output power is consistent with the actual value; when the decision-maker considers the uncertainty of wind and solar, this study sets the initial prediction target deviation coefficient to 0.5; the degree of uncertainty is obtained as $\sigma_{\text{risk}} = 0.142$. Correspondingly, the optimal scheduling schemes of GVPP in deterministic and uncertain scenarios are calculated, respectively. Figure 6 shows the optimal scheduling scheme of GVPP under different prediction target deviation coefficients.

According to Figure 6, if we do not consider the uncertainty of the scenery, to pursue the goal of minimizing the cost of power generation, GVPP will give priority to using WPP and PV for power generation. CGT is mainly used to meet the basic load, and GST, DRP and PSD mainly provide peak shaving services; when considering the uncertainty of wind and solar, to increase the flexibility of the system, CGT began to participate in wind and solar peak shaving. At this time, to reduce the overall cost of power generation, BPG power generation output increased, and P2G converts more CO_2 into CH_4, reducing the carbon

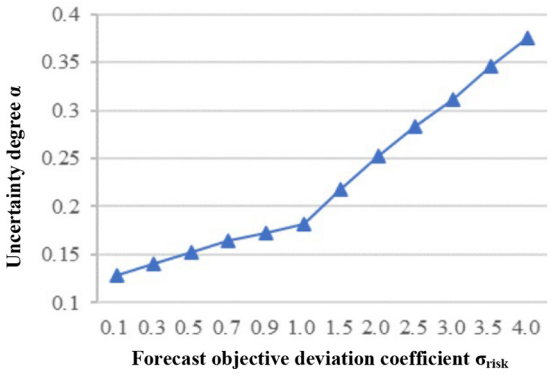

Figure 5.
Relationship between uncertainty degree α and predicted objective coefficients σ_{risk}

emission cost of GVPP, and the range of DRP and PSD calls are significantly increased to improve GVPP's ability to cope with the uncertainty of scenery. Table 1 shows the GVPP scheduling optimization plan under different scenarios.

According to Table 1, when considering the uncertainty of wind and solar output power, the power output of CGT and BPG increased by 4.68 MW·h and 14.64 MW·h, while the output of wind power decreased by 7.88 MW·h. At the same time, because P2G and PSD have the ability to use energy waste during valley hours and supply power during peak hours, DRP has the ability to provide negative output during peak hours. Therefore, to pursue the goal of the lowest power generation cost, PV power generation increases by 1.39 MW·h during peak hours during the day. In addition, when the expected target deviation coefficient is 0.5, the corresponding degree of uncertainty is 0.142. At this time, the carbon emissions have been reduced to 0 tons, that is, zero carbon emissions have been achieved.

In summary, this study proposes to apply the IGDT to the uncertainty of the wind and solar and establishes the GVPP low-carbon random call optimization model. The results of the above calculation examples verify that the optimization results are in line with the actual scheduling experience and reflect the effectiveness of the method in this study. In general, the GVPP low-carbon stochastic scheduling optimization model proposed in this study can reasonably set the expected target deviation coefficient for decision-makers based on their own risk attitudes and then obtain the optimal decision-making plan that meets their own requirements and provide effective decision-making tools.

4.3 Near-zero carbon dispatching plan

Applying the GVPP low-carbon stochastic scheduling optimization model based on the IGDT proposed in this study, this section takes zero carbon emissions from GVPP operations as the goal and calculates the corresponding prediction target deviation coefficient and uncertainty cost. When the predicted target deviation coefficient is equal to 0.326, GVPP achieves near-zero carbon scheduling, and the degree of uncertainty at this

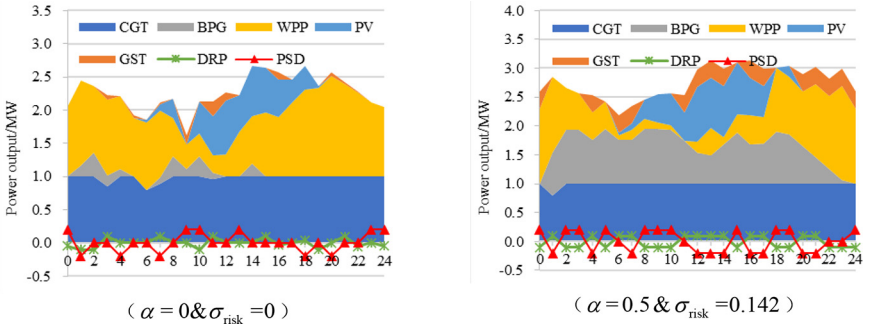

Figure 6.
Dispatching optimization results of GVPP under different object deviation coefficients

Table 1.
Dispatching optimization results of GVPP under different scenarios

Scene	Power generation/MW·h					Regulate output/MW·h		Carbon emission/ton	Target value	
	CGT	BPG	WPP	PV	P2G	PSD	DRP		F_{cost}	σ_{risk}
Certainty	24.32	1.92	22.67	5.58	−1.39	±1	±0.54	13.75	4875.10	0
Uncertainty	28.00	16.56	14.79	6.97	−7.86	±2	±1.2	0	6512.19	0.142

time is equal to 0.131. Figure 7 shows the GVPP optimal dispatch plan under the zero carbon emission scenario and the worst scenario.

According to Figure 7, when the decision-maker expects that the target deviation coefficient is set to 0.326, GVPP operation can reach the critical value of zero carbon emissions. At this time, GVPP can sell carbon emission allowances through the trading market. To achieve the goal of zero carbon emissions, BPG was not used due to high carbon emissions per unit of power generation. Peak shaving services for wind power and PV power generation are mainly satisfied by P2G, PSD and DRP. It is particularly noteworthy that the PSD and DRP operation basically strictly match the peak and valley distribution of the load curve at this time. Further, analyzing the operation of P2G-GST, it can be seen in Figure 8 that P2G mainly converts electricity to gas to generate CH_4 during the low period, most of which are stored in GST, and a small part is directly sold to the gas network. GST inputs natural gas into CGT during peak hours for gas-to-electricity, thereby providing peak shaving output for wind power and PV power generation. Until the end of the dispatch period, the remaining CH_4 is stored in the GST to achieve zero carbon emissions during the dispatch period. Furthermore, the worst scenario established by formulas (37) to (40) is analyzed. Figure 9 shows the GVPP scheduling optimization result under the worst scenario.

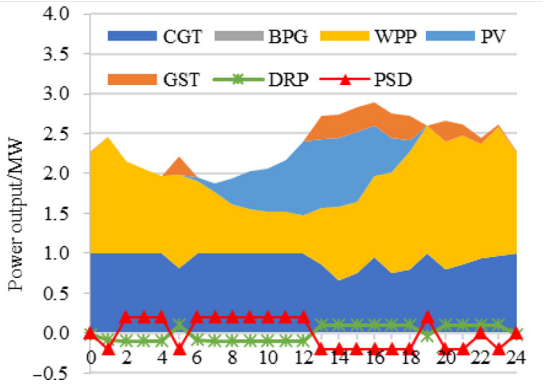

Figure 7.
Dispatching optimization results of GVPP under the zero-carbon emission scenario

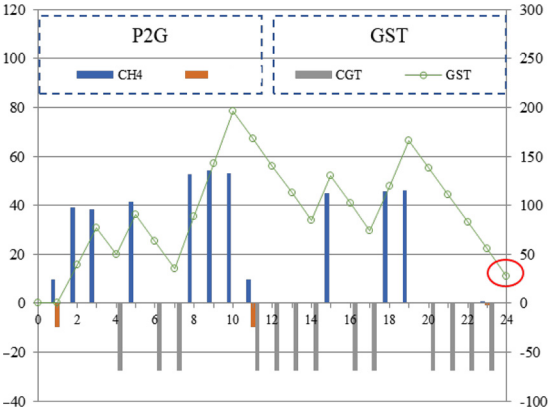

Figure 8.
Operation output of P2G-GST under the zero-carbon emission scenario

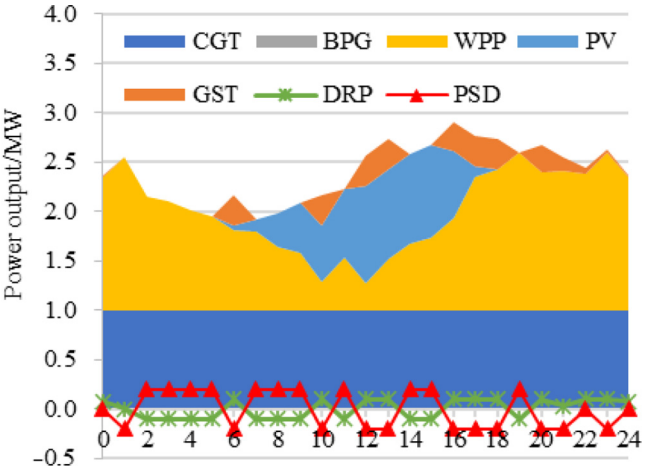

Figure 9.
Dispatching optimization results of GVPP under the worst scenario (α = 0.5 and σ_{risk} = 0.203)

According to Figure 9, in the worst scenario, WPP and PV power generation output is lower than other scenarios significantly. At this time, P2G, PSD and DRP can meet the demand of wind and solar peak shaving, so the CGT power generation output is linear; the output of the upper limit meets the benchmark load demand. Similarly, in pursuit of the objective function of minimizing the cost of GVPP power generation, BPG did not generate power. Different from the zero-carbon emission scenario, in the worst scenario, the PSD and DRP output adjustments are relatively large to deal with the uncertainty of the scenery. Since the output of wind power and PV power generation is the lowest, and BPG is not called, GVPP has a strong ability to deal with the uncertainty of wind power and PV power generation, so the degree of uncertainty σ_{risk} = 0.203; it can be seen that the proposed method can better deal with the worst scenario. Furthermore, the sensitivity analysis of carbon trading prices is carried out. Table 2 shows the cost value and degree of uncertainty of GVPP operations under different carbon trading prices.

According to Table 1, the sensitivity analysis of carbon trading prices is carried out, and the scheduling costs and uncertainty levels of GVPP under certain, near-zero carbon and worst-case scenarios under different carbon trading prices are measured. When the carbon trading price is lower than 50 yuan/ton, the GVPP scheduling cost will decrease as the carbon trading price increases, and the degree of uncertainty will decrease in the near-zero carbon scenario gradually. Since P2G converts more CO_2 into CH_4 and provides greater peak

Table 2.
Operation scheme of GVPP under different carbon price

Carbon trading price	Cost value/¥			Degree of uncertainty σ_{risk}	
	Certainty	Near-zero carbon	The worst scenario	Near-zero carbon	The worst scenario
30	5046.06	5550.67	6310.22	0.121	0.224
35	5009.54	5510.49	6285.07	0.128	0.216
40	4945.35	5439.89	6906.94	0.136	0.210
45	4875.10	6512.19	7585.97	0.142	0.203
50	4811.99	5293.19	8021.27	0.145	0.194
55	4825.08	5307.59	8653.07	0.134	0.187
60	4875.92	5363.51	9733.92	0.129	0.181

shaving capabilities, so GVPP has an increased ability to cope with the uncertainty of the scenery. However, when the carbon trading price is higher than 55 yuan/ton, CGT and BPG generate electricity to generate CO_2, which is used to obtain carbon trading income, which reduces the ability of GVPP to deal with the uncertainty of scenery. For the worst scenario, due to the extremely magnified risk of wind and solar uncertainty, as the price of carbon trading increases, more CGT and BPG power generation will bring higher carbon trading costs. Therefore, the cost of GVPP scheduling is increasing gradually, and the degree of uncertainty is increasing gradually, indicating that the tolerance of decision-makers to the uncertainty of scenery is decreasing gradually. In summary, the actual load dispatch experience of the sensitivity analysis results in Table 2 reflects the effectiveness of the method in this study.

5. Conclusion

This study considers the electrical conversion and spatio-temporal calming characteristics of P2G, integrates it with VPP into GVPP and uses the IGDT to describe the impact of wind and solar uncertainty and then proposes a GVPP near-zero carbon random scheduling optimization model based on IGDT. For different types of decision-makers, the maximum tolerance threshold range of wind and scenery uncertainty can be established by setting the deviation coefficient that meets their own expectations and establish the optimal decision-making scheme of GVPP. By selecting a nine-node energy hub as the simulation system to verify the feasibility and effectiveness of the proposed approach to low GVPP near-zero carbon stochastic scheduling, the following conclusions can be drawn:

- GVPP can coordinate and optimize the output of electricity-to-gas and gas turbines according to the gas-electricity price difference in different periods of the electricity market and natural gas market and use the bidirectional conversion of gas-electricity energy to form an electricity-gas-electricity cycle. It can not only take advantage of the characteristics of VPP to realize the complementary utilization of distributed energy but also improve the system's clean energy absorption capacity through PGST, reduce its own carbon emissions and reduce the volatility of net output.
- The IGDT can be used to describe the impact of wind and solar uncertainty in GVPP. Decision-makers can obtain the maximum tolerance for wind and solar uncertainty by setting a reasonable expected target deviation coefficient. For example, when the expected target deviation coefficient is 0.5, the corresponding uncertainty degree is 0.142. In the worst scenario, the scheduling results obtained by this method are in line with the actual scheduling experience, which reflects the effectiveness of the method in this study.
- Carbon emissions trading can increase the operating space of P2G and reduce the operating cost of GVPP. When the decision-maker expects that the target deviation coefficient is set to 0.326, GVPP operation can reach the critical value of zero carbon emissions, and GVPP can sell carbon emission allowances through the trading market. When the carbon trading price is lower than 50 yuan/ton, the GVPP scheduling cost decreases as the carbon trading price increases, and the degree of uncertainty in the near-zero carbon scenario also decreases gradually, indicating that carbon emissions trading has an important impact on the GVPP scheduling plan.

Note

1. National Development and Reform Commission and National Energy Administration. Notice on Issuing the 13th Five-Year Plan for Energy Development [EB/OL]. www.nea.gov.cn/2017-01/17/c_135989417.htm, 2016-12-26/2020-04-02.

References

Aguilar, J., Bordons, C. and Arce, A. (2021), "Chance constraints and machine learning integration for uncertainty management in virtual power plants operating in simultaneous energy markets", *International Journal of Electrical Power and Energy Systems*, Vol. 133, p. 107304.

Aien, M., Hajebrahimi, A. and Firuzabad, M.F. (2016), "A comprehensive review on un-certainty modeling techniques in power system studies", *Renewable and Sustainable Energy Reviews*, Vol. 57, pp. 1077-1089.

Chaudry, M., Jenkins, N. and Strbac, G. (2008), "Multi-time period combined gas and electricity network optimization", *Electric Power Systems Research*, Vol. 78 No. 7, pp. 1265-1279.

David, F., Florian, K., Raphael, H. and Christopher, V. (2018), "Real live demonstration of MPC for a power-to-gas plant", *Applied Energy*, Vol. 228, pp. 833-842.

Geert, T., Andrej, G., Franz, L., Martin, M., André, B. and Detlef, S. (2018), "Energetically-optimal PEM electrolyzer pressure in power-to-gas plants", *Applied Energy*, Vol. 218, pp. 192-198.

Götz, M., Lefebvre, J., Mörs, F., Koch, A.M., Graf, F., Bajohr, S., Reimert, R. and Kolb, T. (2016), "Renewable power-to-gas: a technological and economic review", *Renewable Energy*, Vol. 85, pp. 1371-1390.

Guandalini, G., Campanari, S. and Romano, M.C. (2015), "Power-to-gas plants and gas turbines for improved wind energy dispatch ability: energy and economic assessment", *Applied Energy*, Vol. 147, pp. 117-130.

Ju, L.W., Tan, Q.L., Lu, Y., Tan, Z.F., Zhang, Y.X. and Tan, Q.K. (2019b), "A CVaR-robust-based multi-objective optimization model and three-stage solution algorithm for a virtual power plant considering uncertainties and carbon emission allowances", *International Journal of Electrical Power and Energy Systems*, Vol. 107, pp. 628-643.

Ju, L.W., Zhao, R., Tan, Q.L., Lu, Y., Tan, Q.K. and Wang, W. (2019a), "A multi-objective robust scheduling model and solution algorithm for a novel virtual power plant connected with power-to-gas and gas storage tank considering uncertainty and demand response", *Applied Energy*, Vol. 250, pp. 1336-1355.

Liu, J., Huang, F.B., Wang, Z.H. and Shuai, C.M. (2021), "What is the anti-poverty effect of solar PV poverty alleviation projects? Evidence from rural China", *Energy*, Vol. 218, p. 119498.

Majidi, M., Mohammadi-Ivatloo, B. and Soroudi, A. (2019), "Application of information gap decision theory in practical energy problems: a comprehensive review", *Applied Energy*, Vol. 249, pp. 157-165.

Manuel, B., Begoña, P., Pilar, L. and Luis, M.R. (2018), "Decision-making methodology for managing photovoltaic surplus electricity through power to gas: combined heat and power in urban buildings", *Applied Energy*, Vol. 228, pp. 1032-1045.

Paolo, C., Giulio, G. and Stefano, C. (2018), "Modelling the integrated power and transport energy system: the role of power-to-gas and hydrogen in long-term scenarios for Italy", *Energy*, Vol. 154, pp. 592-601.

Pilar, L., Guido, F.F., Manuel, B. and Umberto, D. (2018), "Power-to-gas: analysis of potential decarbonization of Spanish electrical system in long-term prospective", *Energy*, Vol. 159, pp. 656-668.

Ting, Q., Huaidong, L., Mianqiao, W., *et al.* (2018), "Low-carbon economic dispatch of electric-heat-gas integrated energy system based on carbon trading", *Power System Automation*, Vol. 42 No. 14, pp. 8-14.

Wang, M., Liu, Y., Shi, W., Li, M. and Zhong, C. (2019), "Research on the remote collaborative sharing strategy of low-carbon technology and emission reduction benefits under the carbon trading policy", *System Engineering Theory and Practice*, Vol. 39 No. 6, pp. 1419-1434.

Wang, Y.Q., Qiu, J., Tao, Y.C., Zhang, X. and Wang, G.B. (2020), "Low-carbon oriented optimal energy dispatch in coupled natural gas and electricity systems", *Applied Energy*, Vol. 280, p. 115948.

Corresponding author
Liwei Ju can be contacted at: jlw@ncepu.edu.cn

For instructions on how to order reprints of this article, please visit our website:
www.emeraldgrouppublishing.com/licensing/reprints.htm
Or contact us for further details: **permissions@emeraldinsight.com**